PAPER

Check for updates

'Leaf vein' inspired structural design of Cu nanowire electrodes for the optimization of organic solar cells†

Xiao Wang, Ranran Wang,* Haitao Zhai, Liangjing Shi and Jing Sun [ID] *

Cu nanowire electrodes have drawn lots of attention recently due to their potential applications in touch panels, organic solar cells and organic light-emitting diodes. The optimization of Cu nanowire electrodes is of great importance in improving the performance of devices based on them. The optical and electrical properties and surface coverage fractions of electrodes composed of nanowires with similar aspect ratios but different geometrical parameters (lengths and diameters) were thoroughly characterized, which enabled the optimization of Cu nanowire electrodes through structural design. Inspired by the grading structure of leaf veins, hybrid Cu nanowire electrodes composed of nanowires with similar aspect ratios but different geometrical parameters were constructed. By combining the advantages of nanowires with various diameters, hybrid Cu nanowire electrodes with improved conductivity at high optical transparency and large effective conducting areas were fabricated. These properties would effectively benefit the effective collection of charge carriers in solar cells. On the basis of these hybrid nanowire electrodes, organic solar cells with enhanced power conversion efficiency were constructed, which cast new light on the optimization of devices based on Cu nanowires.

Introduction

Metal nanowires have attracted ever increasing attention recently due to their excellent conductivity, low cost and easy accessibility.[1–3] The superior conductivity, high optical transparency and excellent flexibility have made metal nanowire electrodes ideal options for constructing organic solar cells (OSCs). OSCs with high power conversion efficiency have been constructed on the basis of metal nanowire electrodes.[4,5] The power conversion efficiency (PCE) of solar cells based on metal nanowires has been reported to be influenced by many factors, such as the conductivity, the uniformity, the surface roughness and the optical performance of metal nanowire electrodes.[5,6] The optimization of metal nanowire electrodes is of great importance for the construction of high performance solar cells.

Structural design has long been regarded as an effective way to optimize of Cu nanowire electrodes. By adjusting the

State Key Laboratory of High Performance Ceramics and Superfine Microstructure, Shanghai Institute of Ceramics, Chinese Academy of Sciences, China.
E-mail: wangranran@mail.sic.ac.cn, jingsun@mail.sic.ac.cn

† Electronic supplementary information (ESI) available: The simulation results of the absorption cross section and scattering cross section of a single LDL nanowire and an SDS nanowire; the illustration of the transportation of electrons in LDL networks, SDS networks and hybrid networks; and the corresponding SEM images of the nanowire electrodes processed with the Image-pro plus software. See DOI: 10.1039/c8tc00114f

geometry or alignment of nanowires, or combining them with other materials, the performance (transmittance, conductivity, surface roughness or the coverage fraction) of nanowire electrodes and the PCE (power conversion efficiency) of solar cells based on them could be significantly optimized.[7,8] A thorough understanding of the influence of structural parameters (diameters and lengths of nanowires) on the performance of nanowire electrodes and solar cells based on them is the foundation for any further structural optimization. In order to understand these influences, experiments and simulations have been carried out. On the basis of the FDTD (Finite-Difference Time-Domain) simulation and experimental results, Wiley *et al.* found that the uniformity of the diameter and length of nanowires would influence the performance of nanowire electrodes. The importance of controlling the length dispersity of nanowires was highlighted.[9] Coleman's research results indicated that nanowires with small diameters were favourable in transparent conducting applications.[10] For the purpose of model simplification, researchers applied nanowires with variable diameters but similar lengths or with variable lengths but similar diameters as research subjects. However, unlike these nanowires obtained through ultrasonic irradiation treatments, the as-synthesized nanowires usually show differences in both diameters and lengths.[11] The influences of diameters and lengths should both be taken into account when considering the performance of nanowire electrodes. Some researchers applied the aspect ratios of metal nanowires as the subject of theoretical simulations to get a clear image.

Nanowires with high aspect ratios were found to be helpful in the optimization of metal nanowire electrodes.[9,10,12,13] However, the fact that nanowires with different geometrical parameters (lengths and diameters) might show similar aspect ratios was neglected. As nanowires with different diameters usually exhibit different optical and electrical properties, differences between theoretical simulation and experimental results still existed, which hindered further structural optimization of metal nanowire electrodes. Taken together, the optical and electrical performance of metal nanowire electrodes could be influenced by the joint effects of the diameters and lengths of nanowires. A comprehensive study on the optical and electrical properties of nanowires with different diameters and lengths is essential for further optimization of nanowire electrodes.

Apart from the conductivity of electrodes at certain transmittance, the effective conducting area is also an important factor in determining the performance of solar cells due to its noticeable impact on the efficiency of charge-carrier-collection.[6] Though exhibiting superior electrical performance compared to other transparent electrodes based on carbon materials or polymers, metal nanowire electrodes have long been criticized for their small effective conducting area. Due to the fact that metal nanowires can only collect the charge carriers generated in their near neighbourhood, a higher density of nanowires would be helpful in improving the photocurrent of solar cells.[6] However, increasing the density of nanowires would severely deplete the transmittance of nanowire electrodes and harm the performance of solar cells. Co-percolate networks with 1D–1D (nanowires with various diameters or metal nanowires–carbon nanotubes) composite structures or 1D–2D (nanowires–graphene) composite structures may effectively resolve the conflicts between the transmittance, the conductivity and the effective conducting area of nanowire electrodes. Pei *et al.*[6] reported a composite electrode which was composed of both short and long Ag nanowires. The embedded networks of long Ag nanowires effectively improved the conductivity of electrodes while the layer of short Ag nanowires helped in improving the effective conducting area of the electrodes. Solar cells with improved photocurrents and power conversion efficiencies were constructed by applying the composite electrodes. However, the average diameters of Ag nanowires applied in the composed electrodes were larger than 60 nm. The addition of short Ag nanowires, which contributed to the formation of percolating conductive paths, severely blocked the light from going through the electrodes. The disadvantages of Ag nanowires with low aspect ratios limited further optimization of the solar cells based on the composite electrodes. Compared with Ag nanowires, single layer graphene shows a higher transmittance of 97.7%, which makes it another candidate for constructing co-percolating networks.[8,14] However, the difficulties in the large-scale fabrication of single layer graphene and the high resistance between graphene and metal nanowires limited its application.

The leaf vein is a typical multi-scale architecture with grading structures perfected by evolution.[15] The combination of primary veins with high lengths and large diameters and lateral veins with short lengths and small diameters enables the transportation of water to every part of a leaf and the effective collection of

photosynthetic products without affecting the absorption of light by photosynthetic cells. This state-of-the-art architecture of leaf veins has inspired numerous structural design masterpieces in many fields.[16] Flexible electrodes have been constructed based on the structure of leaf veins. Gao[17] *et al.* constructed highly conductive and transparent microscaffold networks by coating Ag onto the surface of chemically extracted vein structures. However, due to the intrinsic geometries of leaf veins, the large scale application of electrodes is limited.

For the purpose of solving these aforementioned problems and constructing solar cells with improved performance, a new method for the structural optimization of Cu nanowire electrodes was proposed. Cu nanowires with similar aspect ratios (∼1360) but different diameters and lengths were synthesized by adjusting the species of capping agents utilized in the synthesis process. On the basis of the Cu nanowires synthesized, Cu nanowire electrodes with superior conductivity (FoM ∼ 240) were constructed. A detailed characterization of the optical and electrical performance, surface roughness and coverage fraction properties of electrodes composed of Cu nanowires with different geometrical parameters was carried out. A comprehensive understanding of the properties of nanowires with various geometrical parameters and their electrodes enabled the structural optimization of Cu nanowire electrodes. Inspired by the grading structure and the function of leaf veins, we proposed hybrid nanowire electrodes on the basis of Cu nanowires with similar aspect ratios but different average diameters and lengths. On the basis of these hybrid electrodes, OSCs with improved photocurrent and power conversion efficiency were fabricated. Compared with the OSCs based on the electrodes composed of a single type of Cu nanowires, an increase of 43% in the PCEs was achieved. The advantages of hybrid electrodes in the construction of highly efficient OSCs opened up a new method for the optimization of devices based on Cu nanowire electrodes.

Experimental section

The synthesis of Cu nanowires

Cu nanowires with an average diameter of 120 nm and an average length of 150 μm (LDL nanowires, long nanowires with larger diameters) were synthesized using OLA (oleylamine) as the solvent and reducing agent and CTAB as the capping agent. HDA and CTAB were mixed and melted at a temperature of 190 °C to form a uniform solution. After the addition of Ni(acac)$_2$, the solution was aged at a temperature of 190 °C for an hour. Cu(acac)$_2$ was then added to the solution to form a uniform dark-red solution. Cu nanowires could be got at the bottom of the reaction vessel after 12 h of reaction. Cu nanowires with an average diameter of 25 nm and an average length of 30 μm (SDS nanowires, short nanowires with smaller diameters) were synthesized by a method reported previously.[18] Cu(acac)$_2$, CuCl$_2$, Ni(acac)$_2$ and oleylamine were mixed and aged at a temperature of 80 °C for 20 min to ensure full dissolution of metal salts. The temperature was then raised to

This journal is © The Royal Society of Chemistry 2018

J. Mater. Chem. C, 2018, 6, 5738–5745 | 5739

165 °C to enable the reduction of Cu^{2+} ions. $CuCl_2$ was added to the solution to initiate the formation of Cu nanoseeds and the anisotropic growth of Cu nanowires. Cu nanowires with an average diameter of 24 nm could be got after 4 h of reaction.

The fabrication of Cu nanowire electrodes

Cu nanowires mixed in different proportions were deposited onto the surface of a filter membrane by a vacuum filtration process to form a Cu nanowire network. The network was then transferred to the surface of a glass slide for further characterization and application by a hot-pressing transfer process. During this process, the filter membrane with a Cu nanowire network was placed on a glass slide and kept at 80 °C for an hour in a vacuum oven with a 3 kg weight on the top of the glass slide. The membrane will then be removed using an acetone liquid bath. The network was post-treated by a plasma-induced nanowelding process to form a Cu nanowire electrode with high conductivity.[19]

The fabrication of organic solar cells

Cu nanowire electrodes post-treated by a plasma-induced nano-welding process were transferred to polyacrylate substrates to reduce surface roughness. A PEDOT:PSS (Heraeus, Clevios PH1000) layer was formed on the top of the Cu nanowire films by spin coating (1000 rpm for 45 s). An annealing process was then performed on a hot plate at 130 °C for 10 minutes in a glove box to evaporate the solvent. Pure-phase TiO_2 nanocrystals (anatase) were fabricated by a nonhydrolytic sol–gel route reported previously by Wang *et al.*[20] and dispersed in ethanol. The dispersion was spin-coated (4000 rpm for 60 s) onto the substrate to form the TiO_2 layer. After a 10 minute annealing procedure at 130 °C to evaporate ethanol residues, a 100 nm-thick photoactive layer was formed by spin-coating (600 rpm for 60 s) the solution of $P3HT:PC_{61}BM$ (composed of 20 mg P3HT, 16 mg $PC_{61}BM$ and 1 ml orthodichlorobenzene) onto the substrate. An annealing process was carried out at a temperature of 130 °C for 10 minutes to remove the solvent completely. Finally, the MoO_3 layer and the Ag top electrodes were formed by a thermal evaporation process to accomplish the fabrication of OSCs. The effective area of a solar cell was 0.07 cm^2.

Characterization

The micromorphologies of Cu nanowires and Cu nanowire electrodes were analyzed by field emission scanning electron microscopy (SEM, HITACHI S-4800). The electrical and optical performances of Cu nanowire electrodes were tested using a four-point probe (Loresta-EP MCP-T 360) and a UV-vis spectrometer (Lambda 950, Perkin Elmer). The photocurrent–voltage characterization of organic solar cells was performed using a Keithley 2400 source meter under the simulated AM 1.5G illumination (100 mW cm^{-2}; Oriel Sol 3A Class AAA Solar Simulator, Newport) calibrated with an optical power meter (Newport, 1918-R).

Results and discussion

By applying different capping agents in the reaction system, Cu nanowires with similar aspect ratios but different diameters
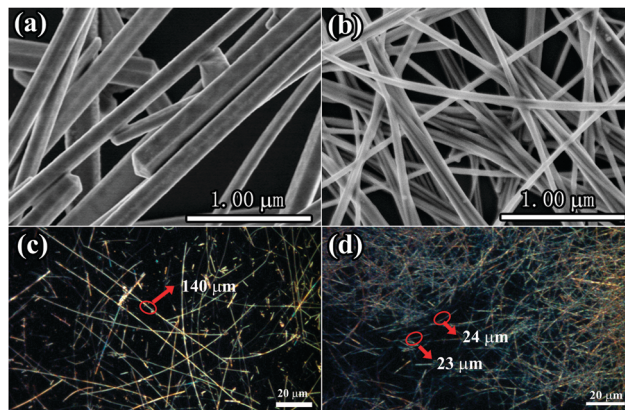

Fig. 1 SEM images of LDL nanowires (a) and SDS nanowires (b); optical microscopy images of LDL nanowires (c) and SDS nanowires (d).

and lengths were synthesized by methods reported in the Experimental section. Oleylamine was used as the solvent and reducing agent, while $Cu(acac)_2$ acted as the metal precursor. $Ni(acac)_2$ was utilized to catalyse the reduction of Cu(ii) ions.[21] When CTAB was applied to enable the anisotropic growth of Cu nanostructures, Cu nanowires with an average diameter of 117 nm and an average length of around 150 μm (LDL nanowires, long nanowires with larger diameters, $L/D \sim 1363$) (calculated from 120 nanowires randomly selected from SEM images) were synthesized (Fig. 1a, c and Fig. S1 in the ESI†). In contrast, the application of Cl^- would lead to nanowires with an average diameter of 20 nm and an average length of 27.3 μm (SDS nanowires, short nanowires with smaller diameters, $L/D \sim 1365$) (calculated from 120 nanowires randomly selected from SEM images) (Fig. 1b, d and Fig. S1 in the ESI†). Compared with CTAB, Cl^- ions could both limit the size of Cu nanoseeds by forming oxidative etching pairs with Cu(ii) ions and promote the anisotropic growth of Cu nanowires, which led to nanowires with smaller diameters.[18] Nanowires synthesized using this organic reaction system exhibited uniform diameters and large aspect ratios, which made them ideal building blocks for nanowire electrodes.

The successful synthesis of high-quality Cu nanowires with tunable diameters provided us with a way to understand the influence of the geometrical parameters of Cu nanowires on their intrinsic properties (the optical and electrical properties) and the performance of nanowire electrodes based on them. For the purpose of understanding the interaction between Cu nanowires with different diameters and the incident light, FDTD simulation was carried out to give the optical properties of single nanowires with different diameters (Fig. 2a and b). Differences could be observed in the calculated transmittance spectra. When placing a SDS nanowire at the center of the simulating field, a flat spectrum with a high optical transparency of 99% was observed. The spectrum of a LDL nanowire exhibited a similar value of 99% at the wavelength ranging from 650 nm to 800 nm. However, a significant decrease of transmittance occurred at a wavelength of 600 nm, which is consistent with the orange-red colour of nanowires. The overall transmittance of

5740 | *J. Mater. Chem. C*, 2018, **6**, 5738–5745

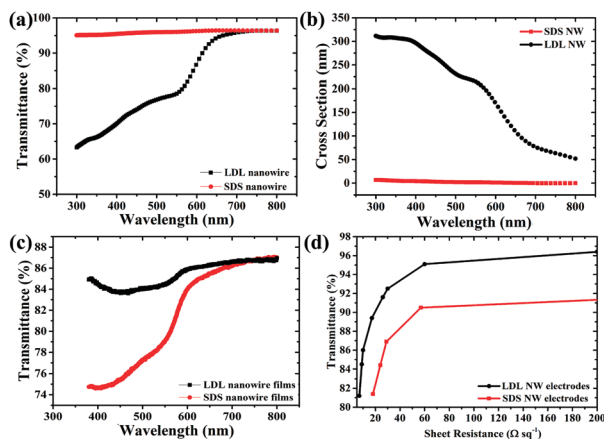This journal is © The Royal Society of Chemistry 2018

Fig. 2 (a) The simulation results of transmittance of a single LDL/SDS nanowire; (b) the simulation results of the extinction cross section of a single LDL/SDS nanowire. (c) The transmittance spectrum of nanowire films with a similar sheet resistance of 15 Ω sq^{-1}; (d) the transmittance and sheet resistance of electrodes composed of nanowires with different diameters and lengths.

the LDL nanowire is nearly 17% less than those of SDS nanowires. In order to understand this difference, we calculated the coverage fraction of each nanowire and compared them with the simulation results. For the SDS nanowire, the coverage fraction was 0.8% (by placing the nanowire in the middle of a 1 μm-wide field), which was similar to the percentage of the light blocked (∼0.35%). However, the coverage fraction of the LDL nanowire (4.8%) (by placing the nanowire in the middle of a 1 μm wide field) was much smaller than the percentage of the light blocked (18.3%). The differences between the coverage fraction and the percentage of the light blocked could be attributed to the light scattering and trapping effect of Cu nanowires.[22] The calculation results shown in Fig. S2 in the ESI† indicated that compared with SDS nanowires, the light absorption ability and light scattering ability of LDL nanowires were much higher, which led to their relatively high cross sections (Fig. 2b) and high light-blocking capacity.

The conductivity of a single Cu nanowire is another important intrinsic property that might be influenced by its geometrical parameters. Previous research results have shown that the resistance of Cu nanowires increased as their diameters decreased,[10,23] which might be caused by the increasing surface and grain boundary scattering of electrons in SDS nanowires.[1]

As nanowire electrodes are usually used to collect and transport charge carriers while allowing light to go through, the conductivity and transmittance of Cu nanowire networks would severely influence the efficiency of OSCs. Cu nanowire electrodes with superior conductivity (low sheet resistance) and high optical transparency could not only enable the effective generation and transportation of charge carriers, but also reduce the current loss at the electrodes, which would greatly improve the PCE of solar cells.[15] The nanowires were then constructed into electrodes to understand the influence of their geometrical parameters (diameters and lengths) on the performance of nanowire electrodes. When comparing the optical

properties of electrodes with similar sheet resistance, a much higher overall transmittance was observed for electrodes composed of LDL nanowires, showing the advantages of LDL nanowires in constructing electrodes with better optical and electrical performance (Fig. 2c). Fig. 2d shows the relationship between the sheet resistance and the transmittance (at a wavelength of 550 nm) of nanowire electrodes. LDL nanowire electrodes showed a lower sheet resistance than SDS nanowires with similar transmittance in the whole range. The figure of merit (FoM = σ_{dc}/σ_{op}) was calculated to characterize the conductivity of nanowire electrodes[3] according to eqn (1). LDL nanowire electrodes showed higher FoMs (FoM ∼ 250) than SDS nanowire electrodes (FoM ∼ 100), which made LDL nanowires better candidates for constructing electrodes with high transmittance and superior conductivity.

$$T = \left(1 + \frac{188.5}{R_S}\frac{\sigma_{op}}{\sigma_{dc}}\right)^{-2} \quad (1)$$

The FoM of nanowire electrodes would be influenced by the following factors: the resistance of nanowires (R_{rod}) and nanowire junctions (R_j), the light-blocking capacity of nanowires and the amount of conducting paths formed in the nanowire network. At high transmittance, the amount of nanowires and conducting paths was limited and resistance (R_{rod} and R_j) played an important role in determining the conductivity of nanowire electrodes. The longer lengths of LDL nanowires could not only improve the efficiency of conducting charge carriers from one side of the network to the other, but also lower the number of nanowire junctions that participate in the transportation of electrons (Fig. S3 in the ESI†). As R_j is much higher than R_{rod},[24] the application of LDL nanowires would effectively minimize the negative effects of nanowire junctions on the conduction of charge carriers and lower the sheet resistance of nanowire networks. Besides, the increment in diameter would lead to a decrease of R_{rod},[1,9,10,23] which would further improve the conductivity of nanowire electrodes. The superior conductivity and high aspect ratio of LDL nanowires resulted in the higher FoM of LDL nanowire electrodes compared with most of the research results reported previously.[21,25] Though exhibiting similar aspect ratios, the shorter lengths of SDS nanowires resulted in a larger amount of junctions in the conducting paths, which was detrimental for the conductivity of the electrodes (Fig. S3 in the ESI†). The differences between LDL nanowire electrodes and SDS nanowire electrodes tended to lessen at a lower transmittance, indicating that the addition of extra LDL nanowires would not contribute to the improvement of FoM as much as SDS nanowires do. This could be easily understood by the compromise between the electrical conductivity and the light blocking capacity of nanowires. The light-blocking capacity of nanowires on the transmittance of the nanowire electrodes started to play an important role in determining the $T\%$–R_s performance of nanowire electrodes. As the extinction cross sections of SDS nanowires are much smaller than those of LDL nanowires, the addition of extra SDS nanowires would form new conducting paths in the nanowire

network without causing much decrease in its light transmittance. These geometrical properties of SDS nanowire networks enable a great increase in the conductivity of thick films.

In addition to transporting electrons, nanowire electrodes also played an essential role in collecting the photo-generated charge carriers. As Cu nanowires could only collect the charge carriers generated in the areas directly connected to them or in their near neighbourhood, the coverage fraction of Cu nanowires would significantly influence the efficiency of charge-carrier collection. According to the research results reported previously, the coverage area of nanowires (A_c) was related to the transmittance of the electrodes in the form shown in eqn (2)

$$\%T = 1 - a_1 100 A_c \qquad (2)$$

In order to simplify the theoretical simulation model, a_1 (the fitting parameter) has been regarded as a fixed parameter (0.87) in many research results reported previously. However, as mentioned above, nanowires with different diameters have different transmittance capacities, and as a consequence, different a_1.[13,22,26] This inconsistency indicated that for nanowire electrodes with similar transmittance, their effective area fraction will differ from each other.

Fig. 3a and b show the SEM images of electrodes with similar transmittance ($\sim 83\%$) but composed of nanowires with different geometrical parameters. Compared with the LDL nanowire electrodes with similar transmittance, the SDS nanowire electrodes exhibited a much denser spatial distribution of conductive areas. The nanowire coverage fraction of electrodes composed of nanowires with different diameters was calculated by processing the SEM images with the Image-pro Plus software (the insets of Fig. 3a, b and Fig. S4 in the ESI†). Compared with LDL nanowire electrodes (16.5%), SDS nanowire electrodes exhibited a much higher nanowire coverage fraction of 28.8% ($T\% \sim 83\%$). The uniform and relatively denser distribution of

conductive areas in SDS nanowires would be favourable in improving the efficiency of charge carrier collection in solar cells. By combining the experimental results with eqn (1), the fitting parameters (a_1) for nanowires with different diameters could be calculated. The a_1 for LDL nanowire electrodes was 1.03, much higher than 0.87. In contrast, SDS nanowire electrodes exhibited a much lower a_1 of 0.59. This result further confirmed that by affecting the optical properties of nanowire electrodes, the geometrical parameters of nanowires would have a great influence on the transmittance of the nanowire electrodes and the distribution of nanowires in them. The coverage fraction for nanowire electrodes with similar transmittance but composed of different nanowires might differ from each other.

Apart from nanowire coverage fractions, the surface roughness of Cu nanowire electrodes is another key parameter that would influence the performance of OSCs. A high surface roughness may lead to shortcuts in solar cells and disable them.[6] In order to maintain the surface roughness of the nanowire electrodes to an ideal range, the nanowire networks were transferred onto the surface of polyacrylate substrates.[19,27] The application of polyacrylate substrates significantly reduced the surface roughness of nanowire electrodes from around 270 nm to around 5 nm (Fig. S5 in the ESI†), which could meet the requirements of OSCs. By embedding the nanowires with polyacrylate substrates during the *in situ* polymerization process, they could be protected from being corroded in the fabrication of solar cells, which enabled the fabrication of highly efficient devices based on Cu nanowire electrodes. The embedding of Cu nanowires led to a smaller coverage fraction of conductive areas (7.5% for SDS nanowire electrodes and 1.5% for LDL nanowire electrodes) (Fig. 3c and d) compared with the actual coverage fraction of nanowires. The distributions of effective conducting areas of electrodes embedded in the polyacrylate substrates were tested by conducting atomic force microscopy (C-AFM). Compared with the electrodes composed of LDL nanowires, SDS nanowire electrodes showed a much more uniform distribution of conducting areas. The large loopholes in the electrodes composed of LDL nanowires would severely limit the performance of solar cells while the application of SDS nanowires could effectively improve the effective coverage area and benefit the charge collection efficiency in solar cells.

As shown above, LDL nanowires and SDS nanowires both have pros and cons in constructing highly efficient OSCs. For electrodes with similar transmittance, the application of LDL nanowires could effectively improve the conductivity of the nanowire electrode and reduce the current loss in electrodes, while electrodes composed of SDS nanowires could collect the charge carriers more effectively due to their higher effective areas. The differences in the optical and electrical properties of LDL nanowires and SDS nanowires provided us with ideal building blocks for the structural design of nanowire electrodes. Inspired by the structure of leaf veins, hybrid Cu nanowire electrodes with grading architectures were constructed to improve the light harvest efficiency and the carrier transfer abilities of OSCs based on them.

LDL nanowires and SDS nanowires were mixed and filtrated to form a hybrid network. SEM images indicated that both
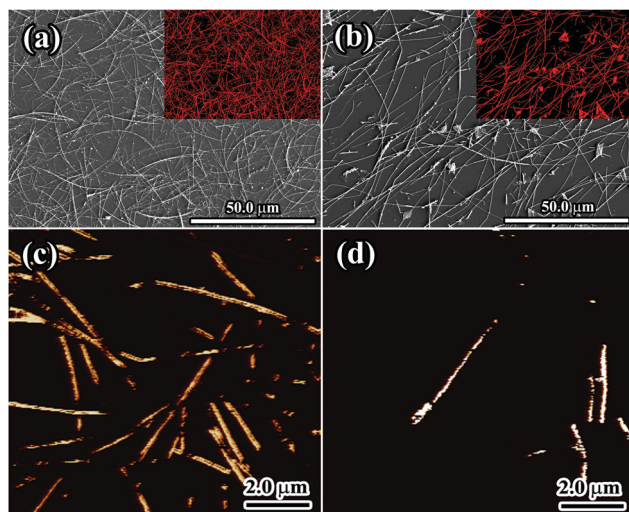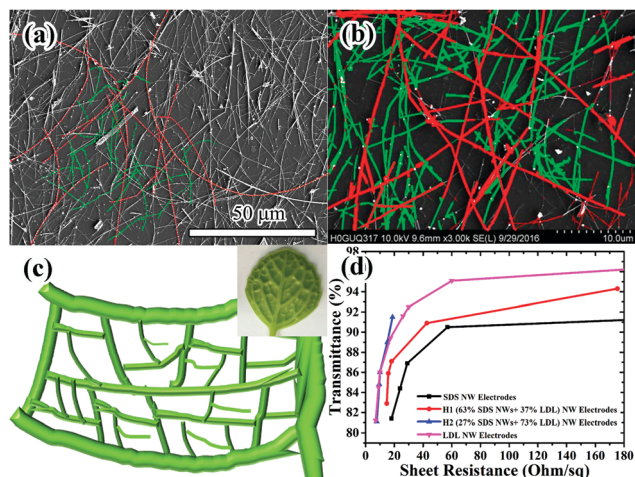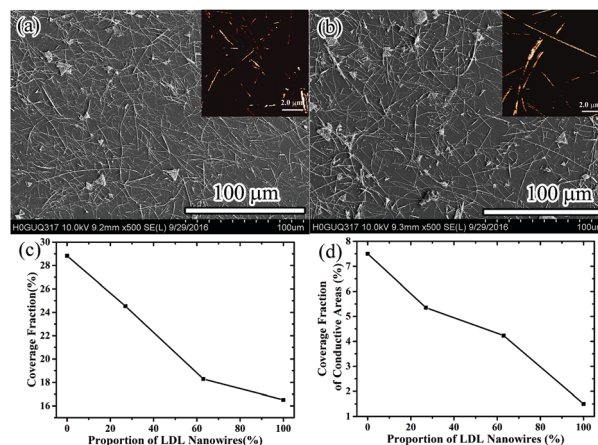

Fig. 3 SEM images of a network composed of SDS nanowires (a) and LDL nanowires (b) ($T\% \sim 85\%$). The insets of (a) and (b) show the corresponding SEM image of the LDL and SDS nanowire electrode processed with Image-pro plus, respectively; C-AFM images of nanowire electrodes composed of (c) SDS nanowires and (d) LDL nanowires ($T\% \sim 85\%$).

Fig. 4 (a and b) The SEM images of a hybrid nanowire network composed of 25% LDL nanowires (highlighted in red lines) and 75% SDS nanowires (highlighted in green lines). (c) Illustration of the collection and transportation of charge carriers in a typical nanowire network. The inset shows the illustration of a typical leaf vein structure. (d) Comparison of the transmittance and sheet resistance of electrodes composed of nanowires with different geometrical parameters.

Fig. 5 SEM images and C-AFM images (insets) of electrodes composed of 27 wt% LDL nanowires and 73 wt% SDS nanowires (H1 electrodes, sample no. 2) (a) and 63 wt% LDL nanowires and 37 wt% SDS nanowires (H2 electrodes, sample no. 3) (b); surface coverage fraction (c) and conductive area fraction (d) of nanowires on the surface of electrodes.

kinds of nanowires distributed uniformly in the hybrid networks. LDL nanowires played the role of the primary veins and formed percolation networks in the electrode while SDS nanowires worked as the lateral veins and fill the holes between LDL nanowires (Fig. 4a, b and Fig. S6 in the ESI†). Just like the structure and function of a typical leaf vein, the LDL nanowires took the primary responsibility of transporting charge carriers, while the SDS nanowires collected charge carriers inside the holes between LDL nanowires and transported them to LDL nanowires (Fig. 4c).

In order to evaluate the morphology and performance of hybrid nanowire electrodes, nanowire networks composed of 27 wt% LDL nanowires and 73 wt% SDS nanowires (H1 electrodes) and networks composed of 63 wt% LDL nanowires and 37 wt% SDS nanowires (H2 electrodes) were constructed and characterized. Fig. 4d shows that compared with nanowire electrodes composed of only SDS nanowires, improved conductivity at a certain optical transparency was achieved by constructing hybrid electrodes. H2 electrodes even showed comparable electrical performance (FoM $\sim$ 240) with the electrodes composed of only LDL nanowires. As shown in the SEM image of hybrid electrodes, LDL nanowires could effectively improve the conductivity of the electrodes by forming percolate networks and overcutting junctions while the addition of SDS nanowires helped in further lowering the resistance with a slight decrease in the transmittance due to their smaller scattering areas (Fig. S2 and Fig. S7 in the ESI†). As the proportion of SDS nanowires increased, the FoM of nanowire electrodes decreased, but it was still higher than electrodes composed of only SDS nanowires (FoM $\sim$ 150 for H1 electrodes *vs.* $\sim$ 100 for SDS nanowire electrodes). The combination of LDL nanowires and SDS nanowires potentiated the construction of nanowire electrodes with high FoMs, which was favorable in the construction of highly efficient OSCs.

In addition to providing high conductivity, the combination of these two kinds of nanowires also helped in improving the coverage fraction and the effective conducting area in an electrode. For electrodes with a similar transmittance of 83%, the coverage fraction calculated from SEM images increased significantly with the increment of the proportion of SDS nanowires (Fig. 5c and Fig. S6 in the ESI†). A larger area fraction and a much denser package of nanowires could be observed. The coverage area fraction was 24.5% for H1 electrodes and 18.3% for H2 electrodes. The distributions of conductive areas in hybrid electrodes were tested by C-AFM. The coverage fraction of the conductive area was calculated using the Image-pro Plus software (Fig. S8 in the ESI†). Compared with electrodes composed of LDL nanowires (the coverage fraction of conducting areas is 1.5%), hybrid electrodes showed a much denser distribution of conductive areas. The coverage fraction of effective conducting areas increased with the proportion of SDS nanowires (5.35% for the H1 electrode and 4.23% for the H2 electrode) (Fig. 5d).

By constructing hybrid nanowire electrodes composed of LDL and SDS nanowires, electrodes with high transmittance, low sheet resistance and dense conductive areas were achieved. These high performance electrodes enabled the fabrication of highly efficient solar cells based on Cu nanowire electrodes. A series of OSCs with a polyacrylate substrate/Cu nanowire network/PEDOT:PSS (PH1000)/TiO_2/P3HT:PC_{61}BM/MoO_3/Ag electrode structure were constructed. As shown in Fig. 6, OSCs based on LDL nanowire electrodes and H2 nanowire electrodes exhibited similar FF and J_{sc}, both higher than the one based on SDS nanowires. FF characterizes the ability of extracting photon-generated charge carriers out of a photovoltaic device.[28] When specific to OSCs based on Cu nanowire electrodes, FF could be influenced by the conductivity and the ability of collecting charge carriers of Cu nanowire electrodes. As mentioned above, SDS nanowire electrodes have larger effective conducting areas when compared with LDL nanowire electrodes. However, the high sheet resistance of SDS nanowire electrodes caused high current
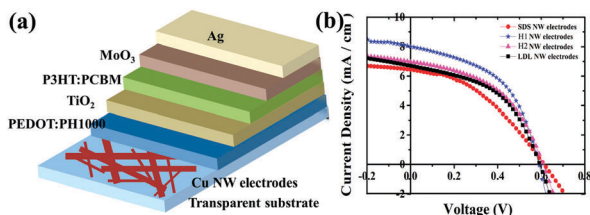
This journal is © The Royal Society of Chemistry 2018

J. Mater. Chem. C, 2018, **6**, 5738–5745 | **5743**

Fig. 6 (a) Schematic illustration of solar cells based on hybrid Cu nanowire electrodes; (b) I–V curves of solar cells based on hybrid Cu nanowire electrodes.

Table 1 Summary of parameters of OSCs based on different Cu nanowire electrodes

Samples	T (%)	R_s ($\Omega\ \square^{-1}$)	V_{oc} (V)	J_{sc} (mA cm^{-2})	FF (%)	PCE (%)
SDS	75.2	12.5	0.594	6.41	39.8	1.56
H1	79.1	11.8	0.591	8.01	49.42	2.33
H2	79.7	10.7	0.601	6.98	48.74	2.06
LDL	80.6	10.8	0.596	6.69	48.6	1.92

loss and harmed the performance of solar cells. Unlike the solar cells based on SDS nanowire electrodes, the ones based on LDL nanowire electrodes exhibited slightly improved performance due to their improved conductivity. However, their limited effective conducting area still held back the fabrication of solar cells with high PCEs. Solar cells with optimized PCEs were obtained when hybrid electrodes were applied. Compared with the electrodes composed of pure SDS or LDL nanowires, the hybrid electrodes exhibited improved T–R_s properties and large effective areas at the same time, which enables the fabrication of OSCs with enhanced J_{sc}, FF and PCEs (Fig. 6b, Table 1 and Table S1 in the ESI†). Though exhibiting a lower transmittance at similar conductivity when compared with H2 electrodes, H1 electrodes showed slight advantages in building organic solar cells due to their larger effective conducting area. Higher FF, J_{sc} and PCEs were observed in the solar cells based on H1 electrodes, which indicated the importance of forming a uniform conducting network and the effective collection of charge carriers in solar cells. The intrinsic flexibility of Cu nanowire electrodes enabled the fabrication of flexible OSCs. The performance of OSCs based on hybrid nanowire electrodes (H1 electrode) remained stable after 500 times of bending (with a bending radius of 3 mm), indicating its possible application in flexible devices (Fig. S9 in the ESI†).

Though exhibiting improved performance, the power conversion efficiency of OSCs with hybrid electrodes was still lower when compared with the ones based on Ag NW electrodes.[29] This could be explained by the reason that Cu nanowires, especially the ones with smaller diameters, are vulnerable to acidic PEDOT:PSS (PH1000), which might be detrimental to the conductivity and the ability of collecting charge carriers of Cu nanowire electrodes. The effective protection of Cu nanowires would be essential for the fabrication of OSCs with improved performance.

Conclusion

On the basis of the grading structure of leaf veins, a new structure was designed for Cu nanowire electrodes. By combining Cu nanowires with similar aspect ratios but different geometrical parameters, hybrid Cu nanowire electrodes with a grading structure were constructed. This new structure provides us with Cu nanowire electrodes with both high conductivity and increased effective conducting area fractions. By applying hybrid Cu nanowire electrodes, organic solar cells with improved PCEs (1.5 times the PCE of the solar cells based on electrodes composed of SDS nanowires) were constructed. We believe that the new structure would create a new vision for the optimization of other devices based on metal nanowires.

Conflicts of interest

There are no conflicts to declare.

Acknowledgements

Notes and references

1 D. S. Hecht, L. Hu and G. Irvin, *Adv. Mater.*, 2011, **23**, 1482.
2 S. Ye, A. R. Rathmell, Z. Chen, I. E. Stewart and B. J. Wiley, *Adv. Mater.*, 2014, **26**, 6670.
3 T. M. Barnes, M. O. Reese, J. D. Bergeson, B. A. Larsen, J. L. Blackburn, M. C. Beard, J. Bult and J. van de Lagemaat, *Adv. Energy Mater.*, 2012, **2**, 353.
4 A. Kim, Y. Won, K. Woo, C.-H. Kim and J. Moon, *ACS Nano*, 2013, **7**, 1081; H. Zhai, R. Wang, W. Wang, X. Wang, Y. Cheng, L. Shi, Y. Liu and J. Sun, *Nano Res.*, 2015, **8**, 3205.
5 B. Y. Wang, T. H. Yoo, J. W. Lim, B. I. Sang, D. S. Lim, W. K. Choi, K. D. Hwang and Y. J. Oh, *Small*, 2015, **11**, 1905.
6 Z. Yu, L. Li, Q. Zhang, W. Hu and Q. Pei, *Adv. Mater.*, 2011, **23**, 4453.
7 H.-Y. Shi, B. Hu, X.-C. Yu, R.-L. Zhao, X.-F. Ren, S.-L. Liu, J.-W. Liu, M. Feng, A.-W. Xu and S.-H. Yu, *Adv. Funct. Mater.*, 2010, **20**, 958; M. Jagota and N. Tansu, *Sci. Rep.*, 2015, **5**, 10219.
8 S. R. Das, S. Sadeque, C. Jeong, R. Chen, M. A. Alam and D. B. Janes, *Nanophotonics*, 2016, **5**(1), 180–195.
9 S. M. Bergin, Y. H. Chen, A. R. Rathmell, P. Charbonneau, Z. Y. Li and B. J. Wiley, *Nanoscale*, 2012, **4**, 1996.
10 S. De, P. J. King, P. E. Lyons, U. Khan and J. N. Coleman, *ACS Nano*, 2010, **4**, 7064.
11 F. Cui, Y. Yu, L. Dou, J. Sun, Q. Yang, C. Schildknecht, K. Schierle-Arndt and P. Yang, *Nano Lett.*, 2015, **15**, 7610; X. Li, P. Zhang, L. Jin, T. Shao, Z. Li and J. Cao, *Environ. Sci. Technol.*, 2012, **46**, 5528; X. Wang, R. Wang, L. Shi and J. Sun, *Small*, 2015, **11**, 4737.
12 K. C. Pradel, K. Sohn and J. Huang, *Angew. Chem., Int. Ed.*, 2011, **50**, 3412; M. Lagrange, D. P. Langley, G. Giusti,

C. Jimenez, Y. Brechet and D. Bellet, *Nanoscale*, 2015, **7**, 17410.

13 S. Sorel, P. E. Lyons, S. De, J. C. Dickerson and J. N. Coleman, *Nanotechnology*, 2012, **23**, 185201.

14 I. N. Kholmanov, C. W. Magnuson, R. Piner, J. Y. Kim, A. E. Aliev, C. Tan, T. Y. Kim, A. A. Zakhidov, G. Sberveglieri, R. H. Baughman and R. S. Ruoff, *Adv. Mater.*, 2015, **27**, 3053.

15 Y. Yu, Y. Zhang, K. Li, C. Yan and Z. Zheng, *Small*, 2015, **11**, 3444.

16 J. Chang, S. Adhikari, T. H. Lee, B. Li, F. Yao, D. T. Pham, V. T. Le and Y. H. Lee, *Adv. Energy Mater.*, 2015, **5**, 1500003; Y. C. Seo, I. You, I. Park, S. S. Kim and H. Lee, *Chem. Mater.*, 2016, **28**, 7990; B. Li, J. Hong, S. Yan and Z. Liu, *Math. Probl. Eng.*, 2013, **2013**, 653895.

17 B. Han, Y. Huang, R. Li, Q. Peng, J. Luo, K. Pei, A. Herczynski, K. Kempa, Z. Ren and J. Gao, *Nat. Commun.*, 2014, **5**, 5674.

18 X. Wang, R. Wang, L. Shi and J. Sun, *J. Mater. Chem. C*, 2018, **6**, 1048.

19 R. Wang, H. Zhai, T. Wang, X. Wang, Y. Cheng, L. Shi and J. Sun, *Nano Res.*, 2016, **9**, 2138.

20 J. Wang, J. Polleux, J. Lim and B. Dunn, *J. Phys. Chem. C*, 2007, **2**, 14925.

21 H. Guo, N. Lin, Y. Chen, Z. Wang, Q. Xie, T. Zheng, N. Gao, S. Li, J. Kang, D. Cai and D. L. Peng, *Sci. Rep.*, 2013, **3**, 2323.

22 C. Preston, Y. Xu, X. Han, J. N. Munday and L. Hu, *Nano Res.*, 2013, **6**, 461.

23 Y. Zhao, Z. Zhang, Y. Zhang, Y. Li, Z. He and Z. Yan, *CrystEngComm*, 2013, **15**, 332.

24 R. M. Mutiso, M. C. Sherrott, A. R. Rathmell, B. J. Wiley and K. I. Winey, *ACS Nano*, 2013, **7**, 7654.

25 L. Dou, F. Cui, Y. Yu, G. Khanarian, S. W. Eaton, Q. Yang, J. Resasco, C. Schildknecht, K. Schierle-Arndt and P. Yang, *ACS Nano*, 2016, **10**, 2600.

26 J. van de Groep, P. Spinelli and A. Polman, *Nano Lett.*, 2012, **12**, 3138.

27 X. Wang, R. Wang, H. Zhai, X. Shen, T. Wang, L. Shi, R. Yu and J. Sun, *ACS Appl. Mater. Interfaces*, 2016, **8**(42), 28831–28837.

28 B. Qi and J. Wang, *Phys. Chem. Chem. Phys.*, 2013, **15**, 8972.

29 L. Mao, Q. Chen, Y. Li, Y. Li, J. Cai, W. Su, S. Bai, Y. Jin, C. Ma, Z. Cui and L. Chen, *Nano Energy*, 2014, **10**, 259–267.